JDI Journal of Diabetes Investigation Open access
Official Journal of the Asian Association for the Study of Diabetes
ORIGINAL ARTICLE

Safflower yellow improves insulin sensitivity in high-fat diet-induced obese mice by promoting peroxisome proliferator-activated receptor-γ2 expression in subcutaneous adipose tissue

Kemin Yan[1], Xiangqing Wang[1], Huijuan Zhu[1], Hui Pan[1], Linjie Wang[1], Hongbo Yang[1], Meijuan Liu[1], Ming Jin[2], Baoxia Zang[2], Fengying Gong[1]*

[1]Key Laboratory of Endocrinology of National Health Commission, Department of Endocrinology, Peking Union Medical College Hospital, Chinese Academy of Medical Science and Peking Union Medical College, Beijing, China, and [2]Department of Pharmacology, China-Beijing Institute of Heart, Lung and Blood Vessel Disease, Beijing Anzhen Hospital, Capital Medical University, Beijing, China

Keywords
Obesity, Peroxisome proliferator-activated receptor-γ2, Safflower yellow

***Correspondence**
Fengying Gong
Tel.: +86-10-6915-5100
Fax: +86-10-6915-5073
E-mail address:
fygong@sina.com

J Diabetes Investig 2020; 11: 1457–1469

doi: 10.1111/jdi.13285

ABSTRACT

Aims/Introduction: Safflower yellow (SY) and its main component, hydroxysafflor yellow A, have been demonstrated to show anti-obesity effects. Peroxisome proliferator-activated receptor-γ2 (PPARγ2) is a critical transcription factor in adipose tissue metabolism. The aim of the present study was to explore the effects of SY in high-fat diet-induced obese mice, and further investigate the mechanism involving PPARγ2.

Methods: High-fat diet-induced obese mice were given 120 mg/kg/day SY for 8 weeks. Glucose and insulin tolerance tests were carried out. Fat mass and serum levels of glucose and insulin were measured. The expression of insulin signaling pathway-related genes and PPARγ2 in the adipose tissue was measured. *In vitro*, the effects of SY (0–500 mg/L) and hydroxysafflor yellow A (0–100 mg/L) on PPARγ2 promoter activities and PPARγ2 messenger ribonucleic acid (mRNA) levels in 3T3-L1 preadipocytes or adipocytes were also detected.

Results: Safflower yellow reduced fat mass, decreased glucose levels and improved insulin sensitivity in obese mice. SY also increased the mRNA levels of insulin signaling pathway-related genes, and increased PPARγ2 mRNA levels by 39.1% in subcutaneous adipose tissue ($P < 0.05$). *In vitro*, SY and hydroxysafflor yellow A significantly enhanced PPARγ2 promoter activities by 1.3–2.1-fold, and increased PPARγ2 mRNA levels by 1.2–1.6-fold in 3T3-L1 preadipocytes or adipocytes ($P < 0.05$).

Conclusions: SY could reduce fat mass, decrease glucose levels and improve insulin sensitivity in high-fat diet-induced obese mice. The probable mechanism is to increase PPARγ2 expression by stimulating PPARγ2 promoter activities, further increasing the expression of insulin signaling pathway-related genes in subcutaneous adipose tissue.

INTRODUCTION

Obesity is a chronic inflammatory disease caused by multiple factors[1]. In 2016, the number of worldwide patients with obesity was >650 million[2]. The prevalence of obesity and its related comorbidities, including cardiovascular disease, type 2 diabetes and cancer, continues to increase. However, drug therapy for obesity remains limited, with side-effects often outweighing benefits[3].

Peroxisome proliferator-activated receptor-γ (PPARγ) is a critical transcription factor in regulating adipogenesis in adipose tissues[4]. PPARγ plays important roles in the regulation of lipids, and glucose metabolism and insulin sensitivity[5–7], and thus is associated with the control of obesity and related diseases[7]. There are two isoforms of PPARγ – PPARγ1 and PPARγ2. PPARγ1 is widely expressed, whereas PPARγ2 is

Received 18 January 2020; revised 24 April 2020; accepted 26 April 2020

predominately expressed in adipose tissue[5,6]. PPARγ is the molecular target of thiazolidinediones (TZDs), which have been used in treating diabetes mellitus for two decades[4]. TZDs have many beneficial effects by improving insulin sensitivity[4]. However, there are many side-effects of TZDs, including bodyweight gain, fluid retention and cardiovascular dysfunction[8,9].

In recent years, traditional Chinese medicine has been reported to possess great potential in treating obesity[10]. *Carthamus tinctorius* L., a member of the Compositae family, is a traditional Chinese medicine with a long history and abundant historical records[11]. The clinical applications of *C. tinctorius* L. included cardiovascular disease[12], cerebral infarction[13], chronic renal failure[14] and so on. *C. tinctorius* L. has also been extensively used in many other Asian countries for treating various diseases[15]. Safflower yellow (SY) is the main component of the flower of *C. tinctorius* L., and hydroxysafflor yellow A (HSYA) is the main active constituent of SY. It has been reported in extensively in the literature that SY and HSYA possess numerous pharmacological effects, including anti-oxidant effects[16], anti-inflammatory effects[17], anti-apoptotic effects[18], cardioprotective effects[19], neuroprotective effects[20] and anti-tumor effects[21,22]. Our previous study found that SY had the anti-obesity effect in high-fat diet (HFD)-induced obese mice[23]. Further investigation showed that the activation of the insulin signaling pathway in adipose tissue, and the browning of white adipose tissue (WAT) might be associated with the beneficial role of SY in obese mice[23]. The investigation in 3T3-L1 preadipocyte found that HSYA could stimulate lipolysis by increasing hormone-sensitive lipase (HSL) messenger ribonucleic acid (mRNA) levels[24]. Consistently, SY was reported by Bao *et al.*[25] to reduce bodyweight and blood lipid levels in mice fed HFD. Liu *et al.*[26] also reported that HSYA could reduce bodyweight, fat accumulation and insulin resistance in HFD-fed mice. However, the detailed mechanism by which SY exerts its anti-obesity effect still needs to be further investigated.

It was shown by Wang *et al.*[27] that HSYA could activate PPARγ in liver tissue to attenuate oxidative stress-induced hepatic fibrosis, and HSYA has also been reported to increase hepatic PPARγ expression in carbon tetrachloride and HFD-induced liver fibrosis rats[28]. However, whether SY has an effect on PPARγ in the adipose tissue have not been reported in previous literature as yet. Adipose tissue has a dominant role in regulating glucose and energy metabolism[29]. Therefore, the purpose of the present study was to explore the effects of SY in HFD-induced obese mice, and further investigate the role of PPARγ2 in adipose tissue or adipocytes after SY or HSYA treatment.

METHODS

Preparation of SY and HSYA

SY was isolated from the water-soluble extracts of the flower of *C. tinctorius* L. by Professor Ming Jin and Professor Baoxia Zang (Beijing An Zhen Hospital, Capital Medical University). SY is composed of a variety of chalcone mixtures. HSYA is the main active component of SY. The concentration of HSYA in the SY is 43.5 g/L (determined by spectrophotometry). The purity of HSYA in the SY is 75.56% (determined by high-performance liquid chromatography, as shown in Figure S1). The chemical compound HSYA (purity 99.4%) was purchased from Chengdu Herbpurify Co., Ltd. (Sichuan, China). The structure and high-performance liquid chromatography analysis of HSYA are shown in Figure S2. The SY was separated using Inertsil ODS-3 column (GL Sciences, Tokyo, Japan) at a flow rate of 0.6 mL/min by the mobile phase composed of methanol–acetonitrile–water (20:10:70) containing 0.02% phosphoric acid. The HSYA was separated using Welch C18 column (Welch, Shanghai, China) at a flow rate of 1.0 mL/min by the mobile phase composed of methanol–acetonitrile–0.5% phosphoric acid water (26:2:72). A main component of SY and HSYA were eluted although the retention time of the main component of SY, and HSYA was different. SY and HSYA were dissolved in deionized water.

Animal experiments

Male ICR mice (8 weeks-of-age, weighing 25–27 g; Beijing HFK Bioscience Co., Ltd, Beijing, China) were randomly assigned to two groups, which were fed with HFD (n = 25) and standard food (SF, n = 10) for 8 weeks, respectively. The SF (H10010, 10% kcal fat) and HFD (H10045, 45% kcal fat) were purchased from Beijing HFK Bioscience Co., Ltd. The compositions of the diets are shown in Table S1. Mice fed with HFD were then randomly divided into the SY group (n = 12) and HFD group (n = 13). The mice were housed in a temperature-controlled room (21–23°C) with a 12-h light–dark cycle, and had free access to water and food. Mice were intraperitoneally injected with 120 mg/kg SY daily in the SY group, and with the same volume of saline in the HFD and SF groups. The bodyweight of mice was recorded weekly. The animal experiments were carried out according to the NIH Guide for the Care and Use of Laboratory Animals. The experimental protocol was approved by the ethics committee of Peking Union Medical College Hospital.

Insulin and glucose tolerance test

The intraperitoneal insulin tolerance test (IPITT) and intraperitoneal glucose tolerance test (IPGTT) were carried out 8 weeks after SY intervention. Mice were intraperitoneally injected with insulin (0.75 U/kg; Novolin R; Novo Nordisk, Copenhagen, Denmark) after they were fasted for 5 h in the IPITT, and with 50% glucose (2 g/kg) after they were fasted for 12 h in the IPGTT. At 0, 30, 60, 90 and 120 min after injection, the blood glucose levels were measured in the tail vein using a glucometer (Roche, Basel, Switzerland). The areas under the curve (AUC) of the IPITT and IPGTT were calculated by the trapezoidal integration[30].

Samples collection and biochemical measurements

Eight weeks after intervention, blood samples of the mice were obtained by eyeball extraction, and centrifuged to extract the

serum samples. Mesenteric WAT (mWAT), epididymal WAT, perirenal WAT, and inguinal subcutaneous WAT (sWAT) were collected and weighed. The adipose tissues were frozen immediately in liquid nitrogen, and then stored at −80°C. A portion of sWAT was fixed in 10% formalin. Histological analysis and the adipocyte size of sWAT were measured, as described previously[31]. Serum fasting blood glucose of mice was measured by routine automated laboratory methods. Fasting serum insulin levels were measured by an enzyme-linked immunosorbent assay kit (Linco Research Inc., St Charles, MO, USA) with an 8.4% intra-assay coefficient of variation. Homeostasis model assessment of insulin resistance (HOMA-IR) was calculated as previously described[32].

Reverse transcription quantitative polymerase chain reaction

Reverse transcription quantitative polymerase chain reaction analysis was carried out in an ABI7500 PCR system (Applied Biosystems, San Francisco, CA, USA) using SYBR® Green Master Mix (Applied Biosystems), as described previously[23] to measure the expression of PPARγ2, forkhead box protein O1 (FOXO1), glycogen synthase kinase 3β (GSK3β), insulin receptor substrate 1 and protein kinase B (AKT). The relative expression of the target gene was calculated by $2^{-\Delta\Delta C_t}$ and normalized to peptidylprolyl isomerase A. The primers sequences were listed in the Table S2.

Cell experiments

The pGL3-Enhancer-PPARγ2 (625 bp)-Luc plasmid, a luciferase reporter gene expression plasmid containing PPARγ2 promoter, was constructed, as in a previous study[32]. 3T3-L1 preadipocytes (obtained from the Department of Genetics, Institute of Life Sciences, Peking University, Beijing, China) were cultured in DMEM with 10% fetal bovine serum at 37°C with 5% CO_2. After seeded in 24-well plates for 24 h, 3T3-L1 preadipocytes were transiently co-transfected with the pGL3-Enhancer-PPARγ2 (625 bp)-Luc plasmid and the pRL-SV40 vector using Lipofectamine 3000 Transfection Reagent (L3000015; Invitrogen, Carlsbad, CA, USA), and treated with 0–500 mg/L SY for 18 h and 100 mg/L SY for 0–36 h. Then the luciferase activities were measured using Dual-Luciferase Reporter Assay System (E1960; Promega, Madison, WI, USA). Renilla luciferase activities were used as the internal control. The relative luciferase activities of SY treated cells were determined by normalization to that of the control cells.

pGL3-Enhancer-PPARγ2 (625bp)-Luc plasmid was stably transfected to 3T3-L1 preadipocytes as described previously[32]. In brief, pGL3-Enhancer-PPARγ2 (625 bp)-Luc and pcDNA3.1 (+) with the neomycin resistance gene were co-transfected to 3T3-L1 preadipocytes using Lipofectamine 2000 Transfection Reagent (L11668019; Invitrogen). Then the monoclonal cells were screened by geneticin (Invitrogen). The luciferase activities were measured as in our previous study[32]. Stably transfected 3T3-L1 preadipocytes were treated with 0–100 mg/L HSYA for 18 h, and with 100 mg/L HSYA for 2–36 h, and then lysed to measure the luciferase activities. The relative luciferase activities of HSYA treated cells were determined by normalization to that of the control cells.

3T3-L1 preadipocytes were cultured in Dulbecco's modified Eagle's medium (DMEM) with 10% fetal bovine serum. At 2 days post-confluence, cells were induced to differentiation in DMEM containing 10% fetal bovine serum, 0.5 mmol/L 3-isobutyl-1-methylxanthine, 10 μg/mL insulin and 10 μmol/L dexamethasone for 48 h, then in DMEM containing 10% fetal bovine serum and 10 μg/mL insulin for 48 h. After that, the medium was replaced to DMEM containing 10% fetal bovine serum every 2 day. Six days later, the differentiated cells were administrated with 50 and 100 mg/L SY for 12, 24 and 36 h, or 100 mg/L HSYA for 24 h, and then total RNA was extracted using E.Z.N.A.® Total RNA Kit II (R6934; Omega Biotek, Norcross, GA, USA), and reverse transcription quantitative polymerase chain reaction analysis was carried out to measure the expression of PPARγ2, adiponectin and uncoupling protein 1.

Statistical analysis

Data are presented as the mean ± standard deviation. Statistical analysis was carried out using SPSS software (version 22; SPSS Inc., Chicago, IL, USA). The univariate analysis of variance (ANOVA) and *t*-test were used for data analysis. Student–Newman–Keuls test was used for two group comparisons. The Kruskal–Wallis test was used if the ANOVA was inapplicable. $P < 0.05$ was considered statistically significant.

RESULTS

SY decreased the fat mass and adipocyte size of sWAT in HFD-induced obese mice

The bodyweight of the mice fed with HFD was significantly increased by 23.5% when compared with the mice fed with SF (54.2 ± 1.4 g vs 43.9 ± 1.1 g, $P < 0.05$), which showed the successful establishment of a HFD-induced obese mice model. During the next 8-week period, the bodyweight of mice in the HFD group was consistently higher than that of the SF group mice (Figure 1a; $P < 0.05$). The total fat mass and fat mass percentage of mice in the HFD group were also increased to 3.2- and 2.4-fold of that in the SF group, respectively (Figure 1b; $P < 0.05$). SY treatment significantly decreased fat mass, although it had no effect on the bodyweight of the obese mice. After SY administration for 8 weeks, the total fat mass and fat mass percentage of the obese mice decreased by 32.5 and 28.7%, respectively (Figure 1b; $P < 0.05$). The mass of sWAT and mWAT of mice in the HFD group were all obviously increased in comparison with mice in the SF group (Figure 1c; $P < 0.05$). After SY treatment, there was a 42.5% reduction in the sWAT mass compared with the HFD group (Figure 1c; $P < 0.05$), whereas there was no significant change in the mWAT mass. Simultaneously, the adipocyte size of the sWAT in HFD group was also increased to 4.0-fold of that in the SF group (Figure 1d-f; $P < 0.05$), and it was also smaller after SY

treatment, which showed a reduction of 46.6% compared with the HFD group (Figure 1d,f,g; $P < 0.05$).

SY improved insulin sensitivity and decreased fasting blood glucose levels in HFD-induced obese mice

As shown in Figure 2, there were higher glucose levels at 0 and 30 min of IPITT in the HFD group than in the SF group (Figure 2a; $P < 0.05$), and the AUC of IPITT in the HFD group was obviously increased to 1.9-fold of the SF group (Figure 2d; $P < 0.05$). After SY treatment, the glucose levels in IPITT at 0, 30 and 60 min were lower than the HFD group (Figure 2a; $P < 0.05$). The AUC of IPITT in the HFD-SY group also decreased to 65.5% of that in the HFD group (Figure 2d; $P < 0.05$), whereas there was no significant difference in the AUC of IPGTT among the three groups. In addition, the fasting blood glucose levels of the mice in the HFD group were markedly increased to 1.5-fold of that in the SF group, and were decreased by 28.1% after SY treatment (Figure 2e; $P < 0.05$). There was no significant change in serum insulin levels among the three groups (Figure 2f). However, HOMA-IR of the HFD group was markedly increased to 2.1-fold of the SF group (Figure 2g; $P < 0.05$). After SY treatment, HOMA-IR showed a trend to decrease compared with the HFD group (4.16 ± 2.08 vs 6.45 ± 4.26, $P = 0.11$).

SY increased the expression of genes involved in insulin signaling pathways in sWAT of HFD-induced obese mice

The mRNA levels of AKT, GSK3β and FOXO1 in the sWAT of mice in the HFD group decreased to 49.3, 67.6 and 36.5% of the mice in the SF group, respectively (Figure 3; $P < 0.05$). After SY administration, the mRNA levels of insulin receptor substrate 1, AKT and GSK3β in the sWAT were obviously increased to 2.9, 1.6 and 1.6-fold of the HFD group, respectively (Figure 3, $P < 0.05$).

SY increased PPARγ2 expression in sWAT of HFD-induced obese mice

The mRNA levels of PPARγ2 in the sWAT and mWAT were measured after SY treatment. In the sWAT, PPARγ2 mRNA levels of the SY-treated mice were notably increased by 39.1% compared with the HFD group (Figure 3e; $P < 0.05$). In mWAT, PPARγ2 mRNA levels showed no significant difference among the three groups (Figure 3f).

SY increased PPARγ2 promoter activities and PPARγ2 mRNA levels in 3T3-L1 preadipocytes and adipocytes

As presented in Figure 4a, 0.01 mg/L of SY remarkably increased the relative luciferase activities to 1.3-fold of the control cells ($P < 0.05$). The relative luciferase activities were increased when SY concentration increased. When the SY concentration increased to 500 mg/L, the relative luciferase activities obviously increased to 1.8-fold of the controls ($P < 0.05$). The results suggest that SY could also promote PPARγ2 promoter activities in a dose-dependent manner. Meanwhile, as shown in Figure 4b, the relative luciferase activities started to increase after 100 mg/L of SY stimulated for 2 h, and the increase continued to 34 h ($P < 0.05$). The relative luciferase activities were maximal to be 1.6-fold of the control cells at 18 h after SY treatment (Figure 4b; $P < 0.05$).

In addition, 3T3-L1preadipocytes were differentiated to adipocytes and treated with SY. As presented in Figure 4c, 50 mg/L of SY significantly increased the PPARγ2 mRNA levels to 1.3-and 1.4-fold of the control cells at 24 h and 36 h, respectively ($P < 0.05$). After 100 mg/L of SY treated for 12, 24 and 36 h, the PPARγ2 mRNA levels of 3T3-L1 adipocytes were also obviously increased to 1.6-, 1.4- and 1.3-fold of the control cells ($P < 0.05$). There was no change in the mRNA levels of adiponectin (Figure 4d) and uncoupling protein 1 (Figure S3) in 3T3-L1 adipocytes after SY treatment.

HSYA increased PPARγ2 promoter activities and PPARγ2 mRNA levels in 3T3-L1 preadipocytes and adipocytes

As shown in Figure 5a, 10 mg/L HSYA remarkably increased the relative luciferase activities of the 3T3-L1 preadipocytes to 1.4-fold of the controls ($P < 0.05$). When the HSYA concentration increased to 100 mg/L, the relative luciferase activities also obviously increased to 1.9-fold of the controls ($P < 0.05$). As shown in Figure 5b, after HSYA stimulation, the relative luciferase activities began to increase at 12 h, and gradually increased with the extension of time ($P < 0.05$). At 26 h after HSYA stimulation, the relative luciferase activities were maximal to be 2.1-fold of the control cells ($P < 0.05$). The increased relative luciferase activities were still 1.6-fold of the control cells at 36 h ($P < 0.05$). The results suggest that HSYA could also dose- and time-dependently promote PPARγ2 promoter activities. In addition, similar to SY, 100 mg/L of HSYA also increased PPARγ2 mRNA levels of 3T3-L1 adipocytes by 20% compared with the controls (Figure 5c; $P < 0.05$).

DISCUSSION

C. tinctorius L. possesses many pharmacological effects, including anti-inflammation, antioxidant, antidiabetic, analgesic, hepatoprotective and antihyperlipidemic effects[15,33]. SY was isolated and purified from the water-soluble extract of the flower of *C. tinctorius* L. The main active component of SY is HSYA. Our present study showed that SY reduced fat mass, decreased glucose levels and improved insulin sensitivity in HFD-induced obese mice, suggesting the anti-obesity effects of SY. Although SY had no effects on the restoration of glucose intolerance in the HFD-SY group, as shown in IPGTT, glucose levels in IPITT at 0, 30 and 60 min, and the AUC of IPITT in the HFD-SY group were significantly decreased. Although serum insulin levels in the HFD-SY group were shown to be comparable to those in the SF and HFD groups, the fasting blood glucose levels in the HFD-SY group were notably decreased and HOMA-IR showed a trend to decrease. These results suggest that SY could improve insulin sensitivity in HFD-induced obese mice with no effect on insulin

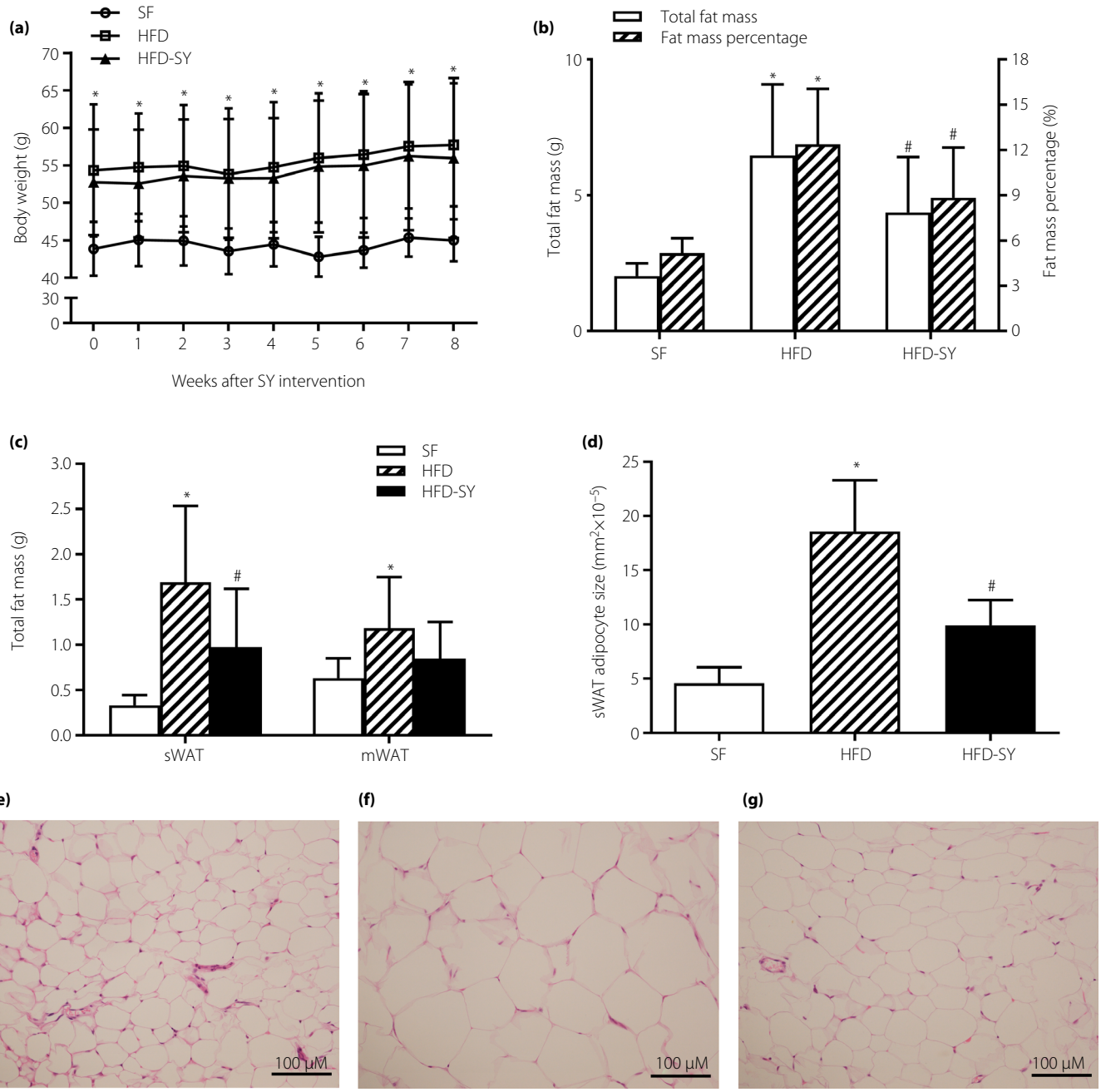

Figure 1 | Effects of safflower yellow (SY) on bodyweight, fat mass and subcutaneous white adipose tissue (sWAT) adipocyte size of high-fat diet (HFD)-induced obese mice. HFD-induced obese mice were treated with SY (120 mg/kg/day) for 8 weeks. (a) The body weight of mice was measured once a week. (b) Eight weeks after intervention, white adipose tissue, including inguinal sWAT, mesenteric WAT (mWAT), epididymal WAT and perirenal WAT, were obtained, weighed and added up to the total fat mass. (b) The fat mass percentage was calculated by the percentage of body weight occupied by the total fat mass. (c) The mass of sWAT and mWAT of mice in the standard food (SF), HFD and SY groups are shown. (d) The adipocyte size of the sWAT of mice in the SF, HFD and SY groups were calculated, as described in the 'Methods' section. Representative hematoxylin–eosin staining of sWAT sections from mice in the (e) SF group, (f) HFD group and (g) SY group at ×200 magnification (scale bars, 100 μm). The data are represented as the mean ± standard deviation. *$P < 0.05$ versus SF group, #$P < 0.05$ versus HFD group ($n = 10$ in the SF group, $n = 13$ in the HFD group and $n = 12$ in the SY group).

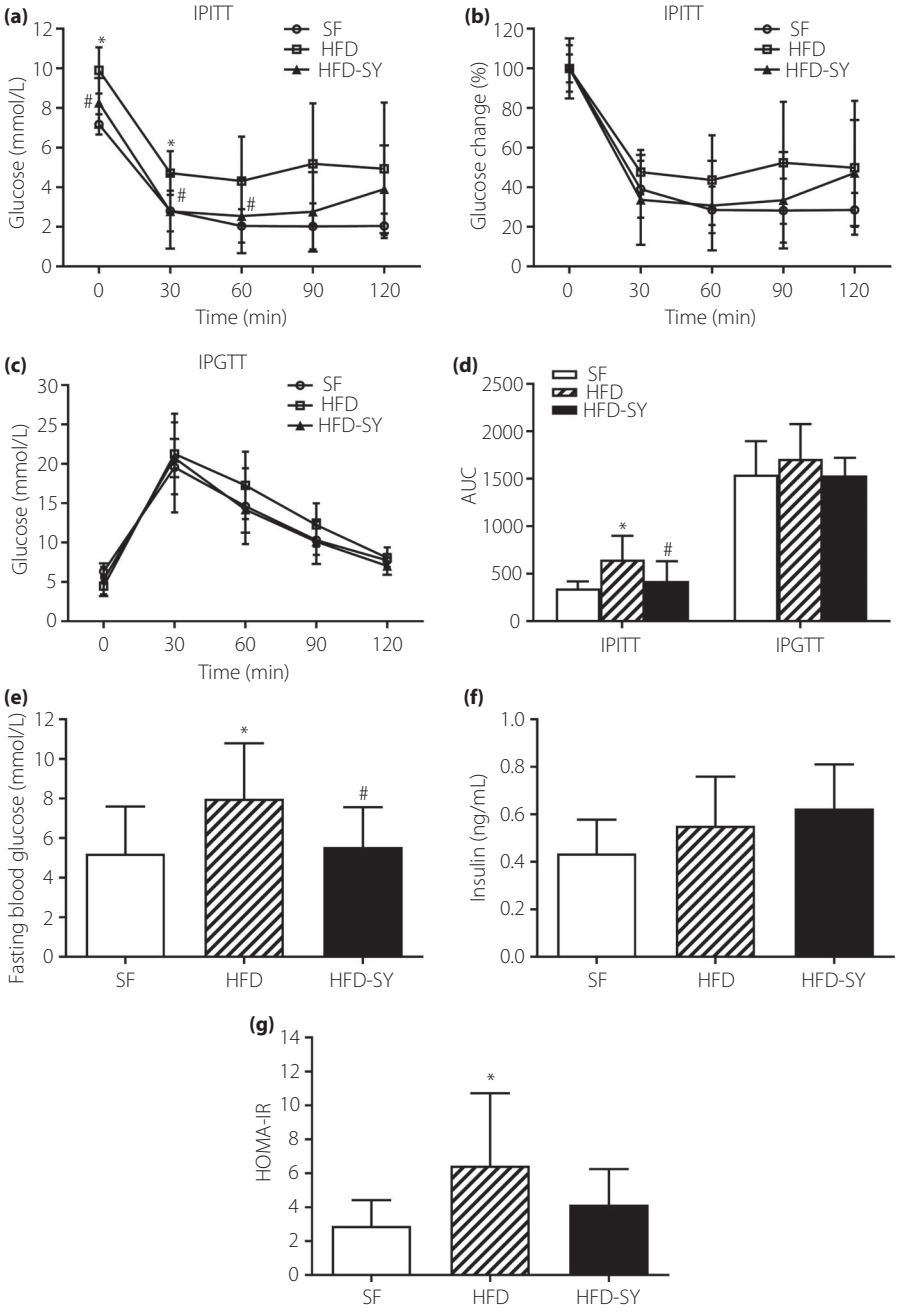

Figure 2 | Effects of safflower yellow (SY) on insulin sensitivity and glucose levels of high-fat diet (HFD)-induced obese mice. HFD-induced obese mice were treated with SY (120 mg/kg/day). Eight weeks after intervention, the (a) intraperitoneal insulin tolerance test (IPITT) and (c) intraperitoneal glucose tolerance test (IPGTT) were carried out in the mice. (b) The data of the IPITT have been normalized to percentage change from the starting glucose levels at T0. (d) Areas under the curve (AUCs) from the IPITT and IPGTT were calculated, as described in the 'Methods' section. Serum levels of (e) fasting blood glucose and (f) insulin were measured, and (g) homeostasis model assessment of insulin resistance (HOMA-IR) were calculated. The data are represented as the mean ± standard deviation. *$P < 0.05$ versus the standard food (SF) group, $^{\#}P < 0.05$ versus HFD group. ($n = 10$ in the SF group, $n = 13$ in the HFD group and $n = 12$ in the SY group).

production. SY improved insulin sensitivity and decreased the fasting blood glucose levels in HFD-induced obese mice, while having no effect on glucose tolerance, showing that the beneficial effect of SY on glucose metabolism was mainly associated with improved insulin sensitivity. In addition, the effect of SY on food intake was investigated in our ongoing

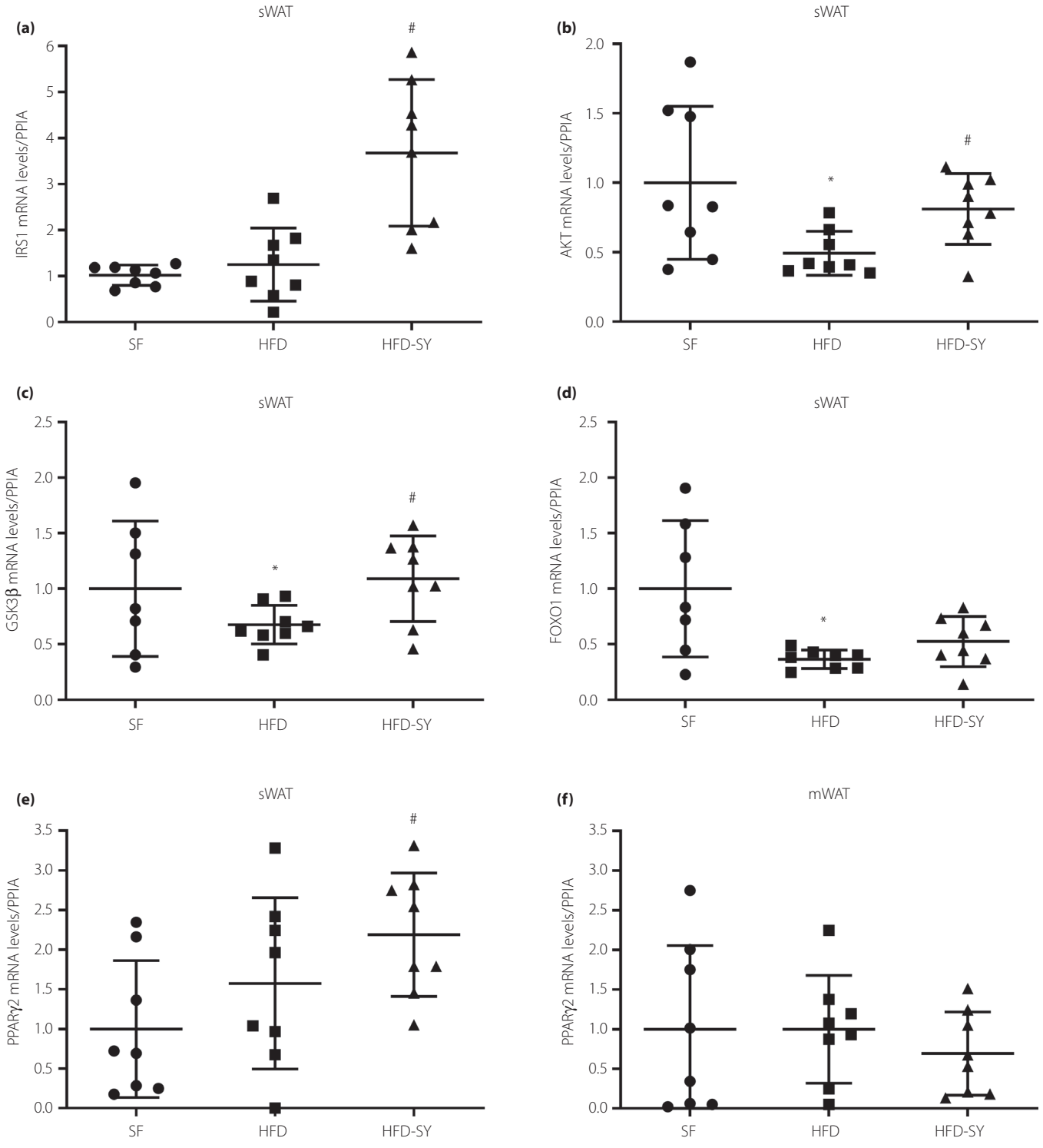

Figure 3 | Effects of safflower yellow (SY) on insulin signaling pathway in subcutaneous white adipose tissue (sWAT) and peroxisome proliferator-activated receptor-γ2 (PPARγ2) messenger ribonucleic acid (mRNA) levels in sWAT and mesenteric WAT (mWAT) of high-fat diet (HFD)-induced obese mice. The (a–d) mRNA levels of insulin signaling pathway-related genes, including (a) insulin receptor substrate 1 (IRS1), (b) protein kinase B (AKT), (c) glycogen synthase kinase 3β (GSK3β) and (d) forkhead box protein O1 (FOXO1), in the sWAT, and PPARγ2 mRNA levels in the (e) sWAT and (f) mWAT of HFD-induced obese mice were determined by reverse transcription quantitative polymerase chain reaction analysis. The *y*-axis represents the quantification of these genes through normalization to peptidylprolyl isomerase A. The data are represented as the mean ± standard deviation. $^{*}P < 0.05$ versus SF group, $^{\#}P < 0.05$ versus HFD group ($n = 8$ for each group). PPIA, peptidylprolyl isomerase A.

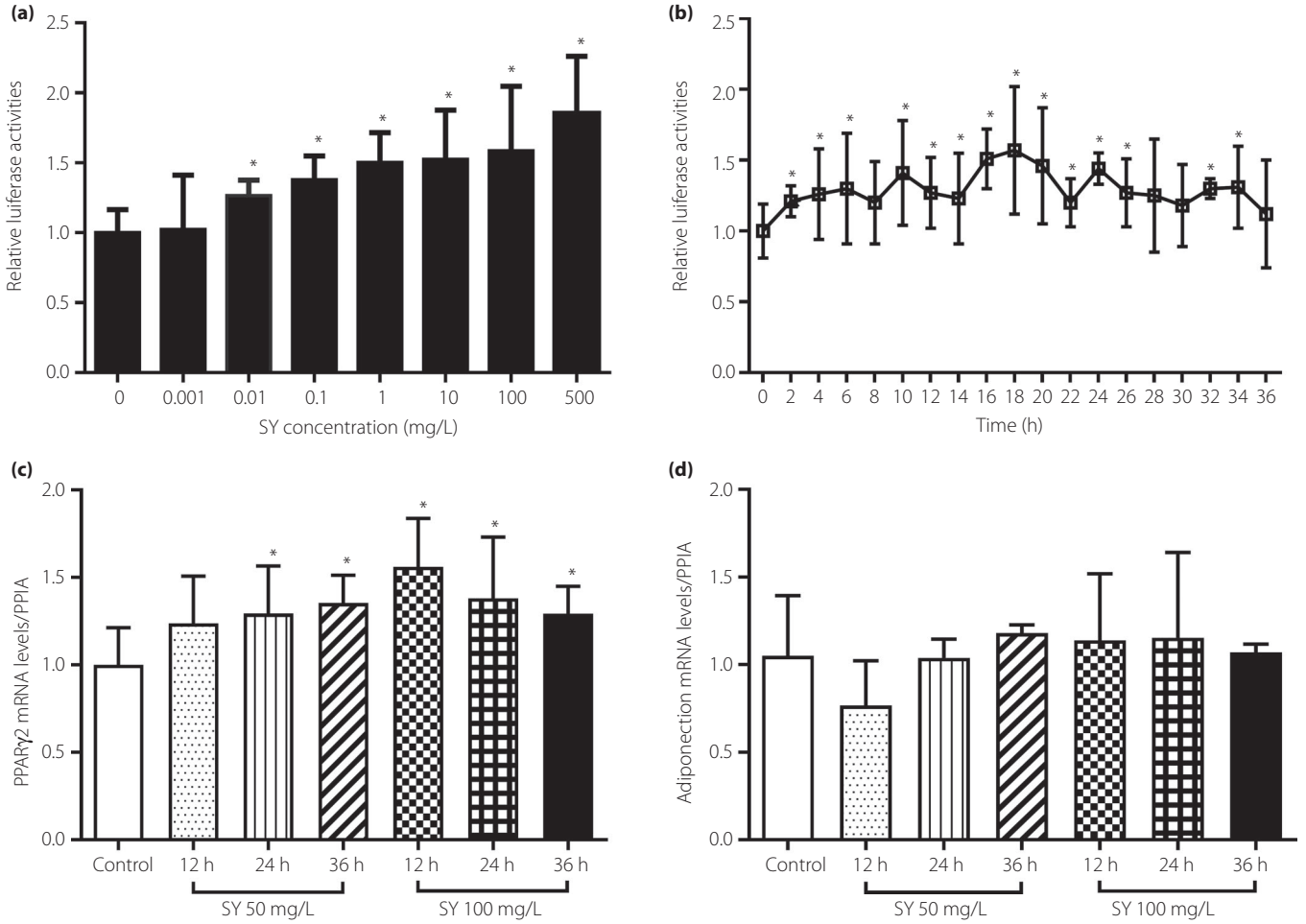

Figure 4 | Effects of safflower yellow (SY) on peroxisome proliferator-activated receptor-γ2 (PPARγ2) promoter activities, and the messenger ribonucleic acid (mRNA) levels of PPARγ2 and adiponectin in 3T3-L1 preadipocytes and adipocytes. 3T3-L1 preadipocytes were transiently co-transfected with the pGL3-Enhancer-PPARγ2 (625bp)-Luc plasmid and the pRL-SV40 vector. The transfected cells were treated (a) with 0–500 mg/L SY for 18 h, and (b) with 100 mg/L SY for 0–36 h. Then cells were lysed and the dual-luciferase reporter assays were carried out. Renilla luciferase activities were used as the internal control. The relative luciferase activities of SY treated cells were determined by normalization to that of the control cells. (c,d) The 3T3-L1 preadipocytes were differentiated to adipocytes. On the 10th day of differentiation, the cells were treated with 50 and 100 mg/L SY for 12, 24 and 36 h. Then total RNA was extracted and reverse transcription quantitative polymerase chain reaction analysis was carried out to measure the expression of PPARγ2 and adiponectin. The data represent the mean ± standard deviation. *$P < 0.05$ versus controls (without SY treatment). PPIA, peptidylprolyl isomerase A.

research, and the result showed no effect of SY on food intake in HFD-induced obese mice (Figure S4).

Accordantly, our previous study and studies carried out by other researchers also showed the anti-obesity effects of SY and HSYA in HFD-induced obese mice[23,25,26]. Previous studies showed that the anti-obesity effect of SY was associated with promoting WAT browning and modulating the gut microbiota[23,26]. In our present study, SY was first discovered to increase the PPARγ2 expression in subcutaneous adipose tissue and adipocytes. Furthermore, treatment with SY and its main active component, HSYA, could directly lead to the stimulation of PPARγ2 promoter activities, resulting in increased PPARγ2 expression. Taken together, we inferred that SY could improve insulin sensitivity in HFD-induced obese mice by promoting PPARγ2 expression in subcutaneous adipose tissue.

PPARγ is the pharmacological target of the insulin-sensitizing agent, TZDs, that decreases insulin resistance and glucose levels in type 2 diabetes patients[34]. PPARγ activation could stimulate the production of small insulin-sensitive adipocytes and increase the expression of insulin signaling pathway-related genes in mature adipocytes to improve insulin sensitivity[35]. The effects of PPARγ on the insulin signaling pathway have been found to directly regulate the expression and phosphorylation of specific insulin signaling pathway related molecules[35]. In the

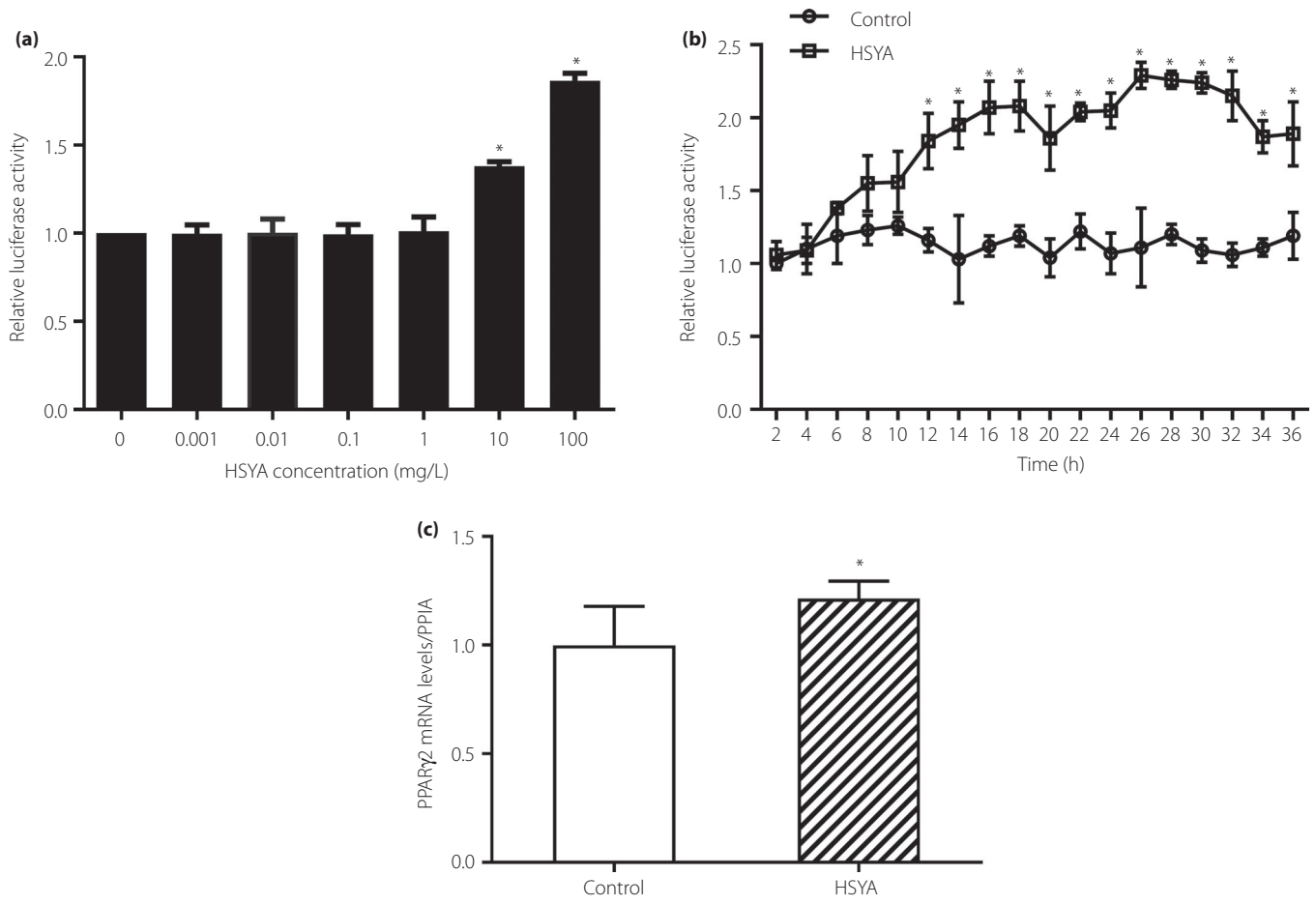

Figure 5 | Effects of hydroxysafflor yellow A (HSYA) on peroxisome proliferator-activated receptor-γ2 (PPARγ2) promoter activities and PPARγ2 messenger ribonucleic acid (mRNA) levels in 3T3-L1 preadipocytes and adipocytes. The 3T3-L1 preadipocytes, which were stably transfected with pGL3-Enhancer-PPARγ2 (625 bp)-Luc plasmid, were plated in 12-well plates and cultured in medium with (a) different concentrations of HSYA (0–100 mg/L) for 18 h, and (b) with 100 mg/L HSYA for different time (2–36 h). Then cells were lysed and the luciferase activities were measured. The relative luciferase activities were obtained in comparison with that of controls. (c) The 3T3-L1 preadipocytes were differentiated to adipocytes. On the 10th day of differentiation, the cells were treated with 100 mg/L HSYA for 24 h. Then total RNA was extracted and reverse transcription quantitative polymerase chain reaction analysis was carried out to measure the expression of PPARγ2. The data represent the mean ± standard deviation of three separate wells in three independent experiments. *$P < 0.05$ versus controls (without HSYA treatment).

present study, SY and its main active component, HSYA, stimulated PPARγ2 promoter activities to increase PPARγ2 expression, which might contribute to the increased expression of insulin signaling pathway-related genes in adipose tissue, thereby improving insulin sensitivity in HFD-induced obese mice. PPARγ agonist has been found to induce fat redistribution from visceral adipose tissue (VAT) to sWAT[36]. It could significantly increase sWAT mass[36,37]. Inversely, in our present study, SY could activate PPARγ2 in sWAT, whereas SY significantly reduced sWAT mass by decreasing the adipocyte size, as well as decreasing the total fat mass. These might result from the lipolysis effect of SY. As shown in our previous study, HSYA, the main active component of SY, could stimulate the lipolysis of 3T3-L1 preadipocytes by increasing HSL promoter activities to increase HSL expression[24]. To clarify the effects of SY on lipolysis, *in vitro* experiments that mainly focused on the effects of SY on HSL expression in the adipocytes differentiated from the primary stromal vascular fraction (SVF) of mice were also carried out. The primary SVF of mice was isolated from subcutaneous and VAT. SY could also increase HSL mRNA levels in the adipocytes differentiated from the subcutaneous SVF, but not in the adipocytes differentiated from visceral SVF (Figure S5a,b). It is well known that there are differential effects of VAT and sWAT on metabolic disease[38]. VAT has been reported to be more insulin-resistant and sensitive to lipolysis than sWAT[39], and more strongly related to the adverse metabolic outcomes[38,40]. Interestingly, in our present study, SY could activate PPARγ2 in sWAT to improve insulin

sensitivity while having no effect on PPARγ2 expression in visceral mWAT. To confirm the effect of SY on the activation of PPARγ2 specifically in sWAT, the effects of SY on PPARγ2 expression in the adipocytes differentiated from the primary SVF of mice were also detected. The results showed that SY could also increase PPARγ2 mRNA levels in the adipocytes differentiated from the subcutaneous SVF, but not in the adipocytes differentiated from visceral SVF (Figure S5c,d). These show that SY could be a novel PPARγ agonist that might selectively activate PPARγ2 in sWAT to improve insulin sensitivity, which could be similar to the selective PPARγ modulators[41]. It was reported by Heitel *et al.*[41] that selective PPARγ modulators activated PPARγ in a tissue-selectivity manner or differentially recruited coactivators to the nuclear receptor in different tissues. It is a specific way for selective PPARγ modulator to tissue-selectively activate PPARγ to achieve insulin sensitization while having slight side-effects[42].

It is well known that adipose tissue inflammation is responsible for insulin resistance in obese individuals. TZDs could enhance adipocyte differentiation, increase the number of smaller adipocytes in the VATs and ameliorate adipose tissue inflammation by activating PPARγ, thereby improving insulin sensitivity[43]. Unlike TZDs, SY significantly reduced fat mass of HFD-induced obese mice, although PPARγ2 mRNA levels were notably increased in the sWAT. SY directly enhanced PPARγ2 mRNA levels in 3T3-L1 adipocytes and the differentiated adipocytes derived from the primary subcutaneous SVF of mice. Additionally, HSYA, the main component of SY, could inhibit the adipogenesis of 3T3-L1 preadipocytes by promoting HSL expression[44]. SY could also increase HSL mRNA levels in the adipocytes differentiated from the primary subcutaneous SVF of mice. Therefore, the mechanism for improvement of insulin sensitivity seems to be a little different in TZDs and SY, although both of them could activate PPARγ2 expression. It is unclear whether SY ameliorates adipose tissue inflammation. A study carried out by Zhang *et al.*[45] showed that SY had beneficial effects on amyloid-β-induced neuroinflammation by inhibiting the release of pro-inflammatory cytokines, nitric oxide synthase and cluster of differentiation 86, in model rats.

In addition, PPARγ activation has been shown to promote browning of WAT[46]. The peroxisome proliferator-activated receptor gamma coactivator 1-alpha (PGC1α)–PPARγ signaling pathway plays an important role in WAT browning. PGC1α is a pivotal transcriptional coactivator that induces WAT browning by activating PPARγ to increase the uncoupling protein 1 transcription[47]. In our previous study, SY significantly increased PGC1α expression in WAT of HFD-induced obese mice[23]. Therefore, the beneficial effect of SY in improving insulin sensitivity could be derived from the activation of the PGC1α–PPARγ signaling pathway and then increasing WAT browning. However, in our present study, SY treatment did not change the mRNA levels of uncoupling protein 1, an important marker of WAT browning. The effects of SY on WAT browning still need to be further studied.

The effects of SY in improving insulin sensitivity might also be relevant to the reduced body fat mass in obese mice. The accumulation of adipose tissue is associated with insulin resistance[48]. Total fat mass and body fat percentage have been shown to strongly correlate with insulin resistance[49,50]. On the contrary, decreasing body fat mass could usefully improve insulin sensitivity. Previous studies carried out with obese people and mice models also discovered that when the fat mass decreased, insulin sensitivity was improved[51,52]. In the present study, SY significantly decreased sWAT mass and total fat mass. Therefore, it could be inferred that SY might also improve insulin sensitivity by decreasing fat mass. Interestingly, SY treatment significantly decreased fat mass, whereas it had no effect on the bodyweight of the obese mice. After careful data analysis, we found that there was a 2.1-g decrease of the average fat mass, and 1.8-g decrease of the average bodyweight. A similar reduction value can be inferred that the weight loss mainly came from the reduction of fat tissue. Of course, the weight increase of other tissues cannot be completely excluded. Unfortunately, we did not measure the weight of other tissues. However, the study carried out by Liu *et al.*[26] in HFD-induced obese mice showed that the administration of HSYA, the main component of SY, had no effect on the weight of liver tissue of mice.

Additionally, the insulin signaling pathway plays an important role in maintaining insulin sensitivity[53]. In detail, insulin sensitivity is associated with a complex network of signaling pathways, including phosphatidylinositol 3-kinase, insulin receptor substrate 1 and insulin-stimulated tyrosine phosphorylation of insulin receptor, as well as AKT serine phosphorylation in the dominant target tissues of insulin, including the adipose tissue, liver and skeletal muscle[54]. Activation of AKT could phosphorylate a number of important downstream effectors, including GSK3β and FOXO1[55,56]. In the current study, the mRNA levels of FOXO1 and AKT in the sWAT were significantly decreased, showing the impairment of insulin signaling pathway in the obese mice. After SY intervention, the impairment of the insulin signaling pathway in the sWAT showed an obvious recovery. The results suggested that SY improved insulin sensitivity by recovering the insulin signaling pathway in adipose tissue of HFD-induced obese mice. The insulin signaling pathways are also modulated by phosphorylation of the insulin signaling molecules. It has been reported in some previous literature that HSYA, the main component of SY, could increase the phosphorylation of AKT in H9c2 cells and in the primary rat brain microvascular endothelial cells[57,58]. HSYA could also increase the phosphorylation of AKT and GSK-3β in H9c2 cells[19]. At this point, some people might be confused that SY decreased the size of subcutaneous adipose tissues although the expression of insulin signaling-related genes was increased, because it is well known that the activation of the insulin signaling pathway of adipocytes can promote glucose uptake and fat synthesis in adipocytes[59]. On this issue, we believed that the increased expression of insulin signaling

pathway-related genes in SY-treated HFD-induced obese mice might result from the decrease of fat mass, because our present *in vitro* study showed that SY could enhance lipolysis by increasing HSL expression (Figure S5) and our previous studies showed that SY could increase WAT browning by increasing PGC1α expression[23], and both might lead to the reduction of fat mass. In our present study, we observed reduced fat mass, increased expression of insulin signaling pathway-related genes and improved insulin sensitivity in SY-treated HFD-induced obese mice. However, the real causal relationship between them needs to be further studied in the future.

In conclusion, SY could reduce fat mass, decrease glucose levels and improve insulin sensitivity in HFD-induced obese mice. The possible mechanism is to increase PPARγ2 expression in sWAT by stimulating PPARγ2 promoter activities, further increasing the expression of insulin signaling pathways-related genes in sWAT, consequently improving the insulin sensitivity of obese mice. The main active ingredient of SY to exert these anti-obesity effects is probably HSYA. Taken together, the present findings provide evidence to highlight SY as a selective PPARγ modulator and a potential compound for the treatment of obesity and type 2 diabetes.

ACKNOWLEDGMENTS

Financial support was provided by the Beijing Natural Science Foundation (Nos. 7182130, 7082079 for FY Gong), the National Natural Science Foundation of China (Nos. 81370898, 30771026, 30540036 for FY Gong, Nos. 81471024, 30600836 for HJ Zhu), the National Key Program of Clinical Science (WBYZ2011-873 for FY Gong and HJ Zhu) and PUMCH Foundation (2013-020 for FY Gong).

DISCLOSURE

The authors declare no conflict of interest.

REFERENCES

1. Heymsfield SB, Wadden TA. Mechanisms, pathophysiology, and management of obesity. *N Engl J Med* 2017; 376: 254–266.
2. WHO.Obesity and overweight, 2018. Available from: http://www.who.int/en/news-room/fact-sheets/detail/obesity-and-overweight Accessed April 1, 2020.
3. Rankin W, Wittert G. Anti-obesity drugs. *Curr Opin Lipidol* 2015; 26: 536–543.
4. Choi SH, Chung SS, Park KS. Re-highlighting the action of PPARgamma in treating metabolic diseases. *F1000Res* 2018; 7: 1127.
5. Anghel SI, Wahli W. Fat poetry: a kingdom for PPAR gamma. *Cell Res* 2007; 17: 486–511.
6. Ma X, Wang D, Zhao W, *et al*. Deciphering the roles of PPARgamma in adipocytes via dynamic change of transcription complex. *Front Endocrinol* 2018; 9: 473.
7. Huang Q, Ma C, Chen L, *et al*. Mechanistic insights into the interaction between transcription factors and epigenetic modifications and the contribution to the development of obesity. *Front Endocrinol* 2018; 9: 370.
8. Choi SS, Park J, Choi JH. Revisiting PPARγ as a target for the treatment of metabolic disorders. *BMB Rep* 2014; 47: 599–608.
9. Bray GA, Smith SR, Banerji MA, *et al*. Effect of pioglitazone on body composition and bone density in subjects with prediabetes in the ACT NOW trial. *Diabetes Obes Metab* 2013; 15: 931–937.
10. Xu L, Zhao W, Wang D, *et al*. Chinese medicine in the battle against obesity and metabolic diseases. *Front Physiol* 2018; 9: 850.
11. Bing X, Yuejun L, Min Y. Literature textual research of the Chinese medicinal Safflower. *Asia-Pac Trad Med* 2018; 14: 58–60 (Chinese).
12. Qiaoying Y, Pingping Y. Clinical observation of safflower injection on 36 angina pectoris patients. *Mod J Integr Tradit Chin West Med* 2002; 11: 581–582 (Chinese).
13. Zhang C. Influence of Honghua injection on effects, blood fat and hemorheology in cerebral infarction patients. *Chin J New Drug Clin Reme* 2001; 20: 273–275 (Chinese).
14. Simei H, Yuliang F, Ronggen C, *et al*. A clinical study on treatment of chronic renal failure with safflower injection by using color Doppler ultrasound. *Chin J Cardiovasc Med* 2001; 6: 215–218 (Chinese).
15. Zhang LL, Tian K, Tang ZH, *et al*. Phytochemistry and Pharmacology of *Carthamus tinctorius* L. *Am J Chin Med* 2016; 44: 197–226.
16. Wang Y, Zhang C, Peng W, *et al*. Hydroxysaf fl or yellow A exerts antioxidant effects in a rat model of traumatic brain injury. *Mol Med Rep* 2016; 14: 3690–3696.
17. Yang XW, Li YH, Zhang H, *et al*. Safflower Yellow regulates microglial polarization and inhibits inflammatory response in LPS-stimulated Bv2 cells. *Int J Immunopathol Pharmacol* 2016; 29: 54–64.
18. Chen L, Xiang Y, Kong L, *et al*. Hydroxysafflor yellow A protects against cerebral ischemia-reperfusion injury by anti-apoptotic effect through PI3K/Akt/GSK3beta pathway in rat. *Neurochem Res* 2013; 38: 2268–2275.
19. Min J, Wei C. Hydroxysafflor yellow A cardioprotection in ischemia-reperfusion (I/R) injury mainly via Akt/hexokinase II independent of ERK/GSK-3beta pathway. *Biomed Pharmacother* 2017; 87: 419–426.
20. Ma Q, Ruan YY, Xu H, *et al*. Safflower yellow reduces lipid peroxidation, neuropathology, tau phosphorylation and ameliorates amyloid beta-induced impairment of learning and memory in rats. *Biomed Pharmacother* 2015; 76: 153–164.
21. Yang F, Li J, Zhu J, *et al*. Hydroxysafflor yellow A inhibits angiogenesis of hepatocellular carcinoma via blocking ERK/MAPK and NF-kappaB signaling pathway in H22 tumor-bearing mice. *Eur J Pharmacol* 2015; 754: 105–114.
22. Fu H, Wu R, Li Y, *et al*. Safflower Yellow prevents pulmonary metastasis of breast cancer by inhibiting tumor cell invadopodia. *Am J Chin Med* 2016; 44: 1491–1506.

23. Zhu HJ, Wang XQ, Pan H, *et al*. The mechanism by which Safflower Yellow decreases body fat mass and improves insulin sensitivity in HFD-induced obese mice. *Front Pharmacol* 2016; 7: 127.
24. Zhu HJ, Wang LJ, Wang XQ, *et al*. Hormone-sensitive lipase is involved in the action of hydroxysafflor yellow A (HYSA) inhibiting adipogenesis of 3T3-L1cells. *Fitoterapia* 2014; 93: 182–188.
25. Bao LD, Wang Y, Ren XH, *et al*. Hypolipidemic effect of safflower yellow and primary mechanism analysis. *Genet Mol Res* 2015; 14: 6270–6278.
26. Liu J, Yue S, Yang Z, *et al*. Oral hydroxysafflor yellow A reduces obesity in mice by modulating the gut microbiota and serum metabolism. *Pharmacol Res* 2018; 134: 40–50.
27. Wang CY, Liu Q, Huang QX, *et al*. Activation of PPARgamma is required for hydroxysafflor yellow A of *Carthamus tinctorius* to attenuate hepatic fibrosis induced by oxidative stress. *Phytomedicine* 2013; 20: 592–599.
28. Liu Q, Wang CY, Liu Z, *et al*. Hydroxysafflor yellow A suppresses liver fibrosis induced by carbon tetrachloride with high-fat diet by regulating PPAR-gamma/p38 MAPK signaling. *Pharm Biol* 2014; 52: 1085–1093.
29. Luo L, Liu M. Adipose tissue in control of metabolism. *J Endocrinol* 2016; 231: R77–R99.
30. Le Floch JP, Escuyer P, Baudin E, *et al*. Blood glucose area under the curve: methodological aspects. *Diabetes Care* 1990; 13: 172–175.
31. Yan KM, Chen WJ, Zhu HJ, *et al*. Ileal transposition surgery decreases fat mass and improves glucose metabolism in diabetic GK rats: possible involvement of FGF21. *Front Physiol* 2018; 9: 191.
32. Yan KM, Zhu HJ, Xu J, *et al*. Lotus leaf aqueous extract reduces visceral fat mass and ameliorates insulin resistance in HFD-induced obese rats by regulating PPARgamma2 expression. *Front Pharmacol* 2017; 8: 409.
33. Asgarpanah J, Kazemivash N. Phytochemistry, pharmacology and medicinal properties of *Carthamus tinctorius* L. *Chin J Integr Med* 2013; 19: 153–159.
34. Nanjan MJ, Mohammed M, Prashantha Kumar BR, *et al*. Thiazolidinediones as antidiabetic agents: a critical review. *Bioorg Chem* 2018; 77: 548–567.
35. Leonardini A, Laviola L, Perrini S, *et al*. Cross-talk between PPARγ and insulin signaling and modulation of insulin sensitivity. *PPAR Res* 2009; 2009: 818945.
36. Laplante M, Festuccia WT, Soucy G, *et al*. Mechanisms of the depot specificity of peroxisome proliferator-activated receptor gamma action on adipose tissue metabolism. *Diabetes* 2006; 55: 2771–2778.
37. Smith SR, De Jonge L, Volaufova J, *et al*. Effect of pioglitazone on body composition and energy expenditure: a randomized controlled trial. *Metabolism* 2005; 54: 24–32.
38. Fox CS, Massaro JM, Hoffmann U, *et al*. Abdominal visceral and subcutaneous adipose tissue compartments: association with metabolic risk factors in the Framingham Heart Study. *Circulation* 2007; 116: 39–48.
39. Ibrahim MM. Subcutaneous and visceral adipose tissue: structural and functional differences. *Obes Rev* 2010; 11: 11–18.
40. Tang L, Zhang F, Tong N. The association of visceral adipose tissue and subcutaneous adipose tissue with metabolic risk factors in a large population of Chinese adults. *Clin Endocrinol* 2016; 85: 46–53.
41. Heitel P, Gellrich L, Heering J, *et al*. Urate transporter inhibitor lesinurad is a selective peroxisome proliferator-activated receptor gamma modulator (sPPARgammaM) in vitro. *Sci Rep* 2018; 8: 13554.
42. Xie X, Chen W, Zhang N, *et al*. Selective tissue distribution mediates tissue-dependent PPARgamma activation and insulin sensitization by INT131, a selective PPARgamma modulator. *Front Pharmacol* 2017; 8: 317.
43. Eggleton JS, Jialal I. Thiazolidinediones. In StatPearls [Internet]. Treasure Island: StatPearls Publishing, 2020. Available from: https://www.ncbi.nlm.nih.gov/books/NBK551656/ Accessed January 20, 2020.
44. Zhu HJ, Wang LJ, Wang XQ, *et al*. Hydroxysafflor yellow A (HYSA) inhibited the proliferation and differentiation of 3T3-L1 preadipocytes. *Cytotechnology* 2015; 67: 885–892.
45. Zhang L, Zhou Z, Zhai W, *et al*. Safflower yellow attenuates learning and memory deficits in amyloid β-induced Alzheimer's disease rats by inhibiting neuroglia cell activation and inflammatory signaling pathways. *Metab Brain Dis* 2019; 34: 927–939.
46. Petrovic N, Walden TB, Shabalina IG, *et al*. Chronic peroxisome proliferator-activated receptor gamma (PPARgamma) activation of epididymally derived white adipocyte cultures reveals a population of thermogenically competent, UCP1-containing adipocytes molecularly distinct from classic brown adipocytes. *J Biol Chem* 2010; 285: 7153–7164.
47. Jankovic A, Golic I, Markelic M, *et al*. Two key temporally distinguishable molecular and cellular components of white adipose tissue browning during cold acclimation. *J Physiol* 2015; 593: 3267–3280.
48. Frayn KN. Adipose tissue and the insulin resistance syndrome. *Proc Nutr Soc* 2001; 60: 375–380.
49. Kurniawan LB, Bahrun U, Hatta M, *et al*. Body mass, total body fat percentage, and visceral fat level predict insulin resistance better than waist circumference and body mass index in healthy young male adults in Indonesia. *J Clin Med* 2018; 7: 96.
50. Zhang M, Hu T, Zhang S, *et al*. Associations of different adipose tissue depots with insulin resistance: a systematic review and meta-analysis of observational studies. *Sci Rep* 2015; 5: 18495.
51. Brachs M, Wiegand S, Leupelt V, *et al*. ANP system activity predicts variability of fat mass reduction and insulin sensitivity during weight loss. *Metabolism* 2016; 65: 935–943.

52. Brandt C, Hansen RH, Hansen JB, *et al*. Over-expression of Follistatin-like 3 attenuates fat accumulation and improves insulin sensitivity in mice. *Metabolism* 2015; 64: 283–295.
53. Pessin JE, Saltiel AR. Signaling pathways in insulin action: molecular targets of insulin resistance. *J Clin Invest* 2000; 106: 165–169.
54. Yaribeygi H, Farrokhi FR, Butler AE, *et al*. Insulin resistance: review of the underlying molecular mechanisms. *J Cell Physiol* 2019; 234: 8152–8161.
55. Sesti G. Pathophysiology of insulin resistance. *Best Pract Res Clin Endocrinol Metab* 2006; 20: 665–679.
56. Guo S. Insulin signaling, resistance, and the metabolic syndrome: insights from mouse models into disease mechanisms. *J Endocrinol* 2014; 220: T1–T23.
57. Hu T, Wei G, Xi M, *et al*. Synergistic cardioprotective effects of Danshensu and hydroxysafflor yellow A against myocardial ischemia-reperfusion injury are mediated through the Akt/Nrf2/HO-1 pathway. *Int J Mol Med* 2016; 38: 83–94.
58. Yang G, Wang N, Seto SW, *et al*. Hydroxysafflor yellow a protects brain microvascular endothelial cells against oxygen glucose deprivation/reoxygenation injury: involvement of inhibiting autophagy via class I PI3K/Akt/mTOR signaling pathway. *Brain Res Bull* 2018; 140: 243–257.
59. Dimitriadis G, Mitrou P, Lambadiari V, *et al*. Insulin effects in muscle and adipose tissue. *Diabetes Res Clin Pract* 2011; 93 (Suppl 1): S52–S59.

SUPPORTING INFORMATION

Additional supporting information may be found online in the Supporting Information section at the end of the article.

Figure S1 | The high-performance liquid chromatography analysis of safflower yellow (SY).

Figure S2 | The structure and high-performance liquid chromatography analysis of hydroxysafflor yellow A (HSYA).

Figure S3 | Effects of safflower yellow (SY) on uncoupling protein 1 (UCP1) messenger ribonucleic acid (mRNA) levels in 3T3-L1 adipocytes.

Figure S4 | Effects of safflower yellow (SY) on food intake of mice.

Figure S5 | Effects of safflower yellow (SY) on the messenger ribonucleic acid (mRNA) levels of hormone-sensitive lipase (HSL) and peroxisome proliferator-activated receptor-γ2 (PPARγ2) in the adipocytes differentiated from the mice primary stromal vascular fraction (SVF).

Table S1 | The compositions of the experimental diets.

Table S2 | Primers for reverse transcription quantitative polymerase chain reaction.